J. Biochem. 2010;147(2):257–264 doi:10.1093/jb/mvp162

JB THE JOURNAL OF BIOCHEMISTRY

Site-directed mutation at residues near the catalytic site of histamine dehydrogenase from *Nocardioides simplex* and its effects on substrate inhibition

Received September 16, 2009; accepted October 4, 2009; published online October 20, 2009

Maiko Tsutsumi, Noriaki Tsuse, Nobutaka Fujieda* and Kenji Kano†

Division of Applied Life Sciences, Graduate School of Agriculture, Kyoto University, Sakyo-ku, Kyoto 606-8502, Japan

*Present address: Department of Material and Life Science, Division of Advanced Science and Biotechnology, Graduate School of Engineering, Osaka University, Suita, Osaka 565-0871, Japan.

†Kenji Kano, Division of Applied Life Sciences, Graduate School of Agriculture, Kyoto University, Sakyo-ku, Kyoto 606-8502, Japan. Tel: +81-75-753-6392, Fax: +81-75-753-6456, E-mail: kkano@kais.kyoto-u.ac.jp

Histamine dehydrogenase from *Nocardioides simplex* (nHmDH) is a homodimer containing one 6-*S*-cysteinyl FMN (CFMN) and one [4Fe–4S] cluster per monomer. nHmDH catalyses the oxidative deamination of histamine to ammonia and imidazole acetaldehyde, but histamine inhibits its catalytic activity at high concentrations. We mutated gene-encoded residues (Tyr180, Gly268 and Asp269) near CFMN to understand the biophysical meaning of the substrate inhibition. Three mutants Y180F, G268D/D269C and Y180F/G268D/D269C were expressed by considering the DNA sequence alignment of histamine dehydrogenase from *Rhizobium* sp. 4-9 (rHmDH), which does not suffer from the substrate inhibition. The Y180F/G268D/D269C mutation to mimic rHmDH successfully suppressed the inhibition, although the catalytic activity decreased. The substrate inhibition was weakened by the Y180F mutation, but G268D/D269C was still susceptible to the inhibition. It was found that it also causes changes in the UV-vis absorption spectra of the substrate-reduced form and the redox potential of the enzymes. The characterization suggests that the thermodynamic preference of the semiquinone form of CFMN in the two-electron-reduced subunit of the enzyme is responsible for the substrate inhibition. However, destabilization of the semiquinone form leads to kinetic hindrance due to the uphill single electron transfer from the fully reduced CFMN to the [4Fe–4S] cluster.

Keywords: histamine dehydrogenase/redox potential/substrate inhibition/6-*S*-cysteinyl flavin mononucleotide/[4Fe–4S] iron-sulfur cluster.

Abbreviations: CFMN, 6-*S*-cysteinyl flavin mononucleotide; $CFMN_O$, the oxidized form of CFMN; $CFMN_S$, the semiquinone form of CFMN; $CFMN_R$, the fully reduced form of CFMN; FeS_O, the oxidized form of [4Fe–4S] iron–sulfur cluster; FeS_R, the reduced form of [4Fe–4S] iron–sulfur cluster; nHmDH, histamine dehydrogenase from *Nocardioides simplex*; rHmDH, histamine dehydrogenase from *Rhizobium* sp. 4–9; TMADH, trimethylamine dehydrogenase.

Histamine dehydrogenase from *Nocardioides simplex* (nHmDH) is an iron–sulfur-containing flavoprotein. nHmDH catalyses the oxidative deamination of histamine to ammonia and imidazole acetaldehyde (*1*). The enzyme is a homodimeric protein composed of subunits with a molecular mass of 76 kDa. Each subunit contains a covalently linked 6-*S*-cysteinyl flavin mononucleotide cofactor (CFMN) and a [4Fe–4S] iron–sulfur cluster. Each subunit also possesses one adenosine diphosphate of unknown function (*2–4*). The DNA sequence alignment shows that nHmDH is closely related to histamine dehydrogenase from *Rhizobium* sp. 4–9 (rHmDH; 64% identical) and trimethylamine dehydrogenase (TMADH; 40% identical), both of which also contain one CFMN and one [4Fe–4S] iron–sulfur cluster per subunit (*3*,*4*).

All these iron–sulfur-containing flavoproteins require three electrons per subunit for full reduction; two for reduction of CFMN and one for the reduction of the [4Fe–4S] cluster. It has been considered that in these enzymes two electrons in the substrate are passed to the oxidized CFMN ($CFMN_O$) and two sequential single electron transfers occur from the fully reduced CFMN ($CFMN_R$) to the oxidized [4Fe–4S] cluster (FeS_O), and finally another two sequential single electron transfers are followed from the reduced [4Fe–4S] cluster (FeS_R) to electron acceptor. The physiological electron acceptor is electron transferring flavoprotein (ETF) for TMADH (*5*), but not identified for nHmDH and rHmDH. Several artificial electron acceptors such as phenazine methosulfate (with dichlorophenolindophenol) (*6*), phenazine ethosulfate (PES) (with DCIP) (*7*) and ferricenium hexafluorophosphate (Fc^+) (*8*) may be utilized in place of the physiological one. Even artificial electron acceptor cannot receive the electron from the reduced flavin site at least in nHmDH and TMADH (*8*). The enzyme kinetics is strongly influenced by the electron acceptor used. In this article, the argument on the effect of the electron acceptor will be minimized for simplicity.

The unique redox properties of nHmDH are observed during the reductive titration with histamine. In the reductive titration with histamine, two-electron reduction occurs per subunit of the enzyme at $pH < 9$, while single-electron reduction occurs at $pH > 9$ (*9*). In the following, we will define the number of electron and the amount of histamine added as those

per subunit. Therefore, the enzyme reduced with one equivalent amount of histamine per subunit corresponds to the enzyme composed of the two-electron-reduced subunits. The two-electron-reduced form of nHmDH subunit is in equilibrium between two ultimate states: one involves the semiquinone form of CFMN ($CFMN_S$) and FeS_R and the other involves $CFMN_R$ and FeS_O (*9*). The distribution is controlled by individual redox potentials which are the function of pH (*9*).

Both nHmDH and rHmDH show high substrate specificity towards histamine. Secondary and tertiary amines including biogenic amines such as tyramine do not react with the enzymes (*1*, *10*). Therefore, the enzymes can be utilized in histamine analysis in food and clinical analysis (*11–13*). nHmDH is much higher in the catalytic activity than rHmDH, but is strongly susceptible to substrate inhibition from histamine at high concentrations. Similar substrate inhibition is also observed for TMADH, which is inhibited by its natural substrate trimethylamine (*7*, *8*, *14*). In contrast, rHmDH does not suffer from such substrate inhibition (*10*).

X-ray crystallographic analysis and sequence alignment have revealed that the amino acid residues near the catalytic site responsible for the substrate recognition and the catalytic reaction are highly conserved, but some residues are different from one another (Fig. 1). In a previous paper, we suggested the importance of three amino acid residues: Trp266 (aromatic bowl which accommodates the substrate by cation-π bonding (*15*), Ser270 and Phe567, for the substrate recognition of nHmDH from the homology modelling of the 3D structure (*3*). The imidazole ring of histamine might be stabilized via hydrogen-bond formation with the hydroxyl group of Ser270 and π interaction with the aromatic groups of Trp266 and Phe567. rHmDH has the corresponding Trp and Ser residues (Fig. 1, Trp263 and Ser267), but only the corresponding Phe residue is replaced with Leu567. It has been proposed that Tyr169, His172 and Asp267 form a catalytic triad in TMADH (*16–18*), and the three amino acids were conserved in nHmDH (Fig. 1, boxed). It has been shown that the catalytic center of nHmDH considerably resembles that of rHmDH, but there are some differences especially at the 180, 268 and 269 positions in the vicinity of CFMN (closed circles, Fig. 1). The amino acid in TMADH and nHmDH of 180 position is conserved, but Phe in rHmDH. In addition, the position of Asp265 in rHmDH, which perhaps forms a catalytic triad, is different from that of the corresponding one in TMADH (Asp267) and nHmDH (Asp269). In order to study whether the differences are responsible for the substrate inhibition characteristics, three mutant proteins of nHmDH involving a single mutation (Y180F), double mutation (G268D/D269C) and triple mutation (Y180F/G268D/D269C) as well as recombinant wild-type (WT) were expressed and characterized in view of enzymatic kinetics, spectroscopy and electrochemistry.

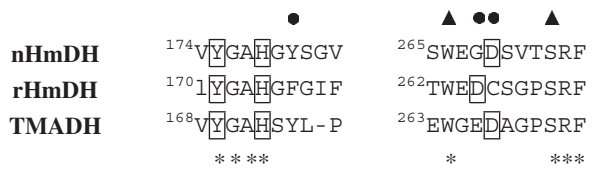

Fig. 1 Amino acid sequence alignment around CFMN of nHmDH, rHmDH and TMADH. nHmDH, *Nocardioides simplex* histamine degydrogenase; rHmDH, *Rhizobium* sp. 4-9 histamine dehydrogenase; TMADH, bacterium W_3A_1 trimethylamine dehydrogenase. Asterisks indicate amino acid residues which are conserved among the aligned sequences. Closed triangles indicate the amino acid residues concerning substrate specificity and the catalytic reaction, which were reported in references (*3*,*10* and *18*). Putative catalytic triad is boxed. Closed circles indicate the amino acid residues mutated in nHmDH and its homologous ones in rHmDH and TMADH.

Experimental procedures

Mutagenesis and expression of nHmDH mutants

Techniques for restriction enzyme digestions, ligation transformation and other standard molecular biology manipulations were based on the methods previously described (*19*) and in part in accordance with the manufacturer's instructions.

The DNA fragment coding for Y180F mutant enzyme (Y180F) was generated by the Quikchange method using plasmid pGEM-*hmd* (*3*, *19*) as a template for KOD-plus polymerase with the primers (forward) 5′-GTGTACGGCGCACACGGCTTCAGCGGCGTC-3′ and (reverse) 5′-GACGCCGCTGAAGCCGTGTGCGCCGTA CAC-3′. The DNA fragments coding for G268D/D269C mutant enzyme (G268D/D269C) and for Y180F/G268D/D269C mutant enzyme (Y180F/G268D/D269C) were generated by the Quikchange method using plasmid pGEM-*hmd* and pGEM-*hmd*Y180F as templates, respectively, for KOD-plus DNA polymerase with the primers (forward) 5′-GGCAGCTGGGAGGACTGCTCCGTCAC GTCC-3′ and (reverse) 5′-GGACGTGACGGAGCAGTCCTCCC AGCTGCC-3′. The final PCR products were gel purified and digested with *Dpn* I. Each of the purified PCR products was digested with *Nde* I and *Hind* III and inserted into pET-26b(+) (Novagen) to yield the expression construct pET-*hmd*Y180F, pET-*hmd*/G268D/D269C or pET-*hmd*Y180F/G268D/D269C, respectively.

Expression and purification of nHmDH mutants

The nHmDH mutants were expressed in *Escherichia coli* strain Rosetta (DE3) and purified as described previously (*19*). Each protein concentration was determined using a modified Lowry method with DC Protein Assay Kit (Bio-Rad, USA) with bovine serum albumin as the standard protein. All chemicals used in this study were of analytical reagent grade and all solutions were prepared with distilled water.

UV-vis spectroscopy

Measurements were performed with a quartz cuvette of a 1-cm light path at a final volume of 2.5 ml under anaerobic conditions at 30°C using a water-jacket cell holder and a thermostat. UV-vis spectra were obtained on a Shimadzu UV-2500PC UV-vis recording spectrophotometer (Japan). Histamine dihydrochloride, agmatine sulfate and putrescine were purchased from Sigma, Wako and Nacalai, respectively, and used as substrates. The nHmDH solutions were prepared at concentrations of 2.6–3.5 μM in a 100 mM potassium phosphate buffer, pH 7.5. The nHmDH solutions were kept anaerobic by repeated evacuation and flushing with O_2-free moisturized argon. The spectra of the reduced forms were taken 3, 15 and 60 min after the addition of histamine, agmatine and putrescine.

Steady-state kinetic measurement

Measurements were performed with a quartz cuvette of a 1-cm light path at a final volume of 3 ml under anaerobic conditions at 30°C using a water-jacket cell holder and a thermostat. Fc^+ was obtained from Aldrich and used as an artificial electron acceptor, because its redox potential is sufficiently positive than that of the enzyme. Each of stock solutions of substrate and Fc^+ was added to the assay mixture to reach desired concentrations. Assays for the determination of kinetic parameters were performed in a 0.1 M potassium phosphate

buffer of pH 7.5. The reactions were initiated by the addition of the enzymes and the decrease in the absorbance at 617 nm due to the reduction of Fc^+ was measured using a Shimadzu UV-2500PC UV-vis recording spectrophotometer (Japan) (*20*). The enzyme kinetics was analysed by a non-linear least-squares method in accordance with the following equation (*21*):

$$\frac{v}{[E]} = \frac{k_{cat}}{1 + \frac{K_S}{[S]} + \frac{[S]}{K_i}} \quad (1)$$

where k_{cat}, K_S and K_i are the catalytic constant, the Michaelis constant of the substrate and the inhibition constant of the corresponding substrate, respectively, and were optimized as adjustable parameters to fit Eq. (1) to the data. [E] and [S] denote the concentration of the enzyme and substrate, respectively.

Spectroelectrochemistry

Mediated spectroelectrochemical titrations for the redox potential measurement of the enzymes were performed by controlling the solution potential in a quartz cuvette using a Hokuto Denko HSV-100 potentiostat (Japan). Absorption spectra were recorded simultaneously on a Shimadzu UV-2500PC UV-vis spectrophotometer as described previously (*9*, *22*). Two osmium complexes, $[Os(bipyridylamine)_2Cl_2](PF_6)_2$ and $[Os(4\text{-imidazole carboxylic acid})_2(bipyridylamine)_2](PF_6)_2$, were synthesized according to the literature (*23*) and used as mediators of the redox titration. The electrolysis solution was a 0.1 M Britton and Robinson buffer containing 5–10 μM nHmDH, 35 μM $[Os(bipyridylamine)_2Cl_2](PF_6)_2$ and 43 μM $[Os(4\text{-imidazole carboxylic acid})_2(bipyridylamine)_2](PF_6)_2$, pH 7.5, at a total volume of 1.7 ml. An antifoaming reagent (Antifoam PE-L, Wako, Japan) was added to the electrolyte solution to a final concentration of 0.3% (w/w). When the spectra became independent of the electrolysis time (i.e. when the solution potential became identical with the electrode potential), the UV-vis spectra were measured. The electrode potential was changed stepwise at several given values. All these experiments on spectroscopy and electrochemistry were performed in a COY Laboratory Products Model A glove box (USA). The concentration of O_2 in the glove box was maintained less than 10 ppm at 30°C.

Cyclic voltammetry

Cyclic voltammetry was carried out on a three-electrode system using a BAS CV-50 W electrochemical analyser (Japan) under anaerobic conditions. A platinum wire and Ag|AgCl|saturated KCl were used as reference and counter electrodes, respectively. The working electrodes used were indium tin oxide (ITO) electrodes (5 × 5 mm, BAS) (*9*). The electrolysis solution was a 0.1 M Britton and Robinson buffer containing 50–70 μM nHmDH and 0.2 M NaCl, pH 7.5, at a total volume of 1 ml. All potentials are referred to the standard hydrogen electrode in this article.

Results

Enzyme kinetics

nHmDH is highly selective to primary amine substrates. Histamine is the best substrate but very small reactivity is observed for agmatine and putrescine (*1*, *2*, *4*). Figure 2A shows the histamine concentration dependence of the steady-state enzyme kinetics (v) for WT and the three mutants (Y180F, G268D/D269C and Y180F/G268D/D269C) in the presence of Fc^+ as an artificial electron acceptor at pH 7.5 and 30°C. The enzyme kinetics exhibited a standard Michaelis–Menten-like dependence on the Fc^+ concentration (data not shown). For simplicity (that is, in order to minimize the effect of the electron acceptor), the Fc^+ concentration was kept as excess (0.33 mM) in the following. On the other hand, histamine showed strong substrate inhibition against WT, as shown by the closed circle. The G268D/D269C mutant (indicated by the closed triangle) was also

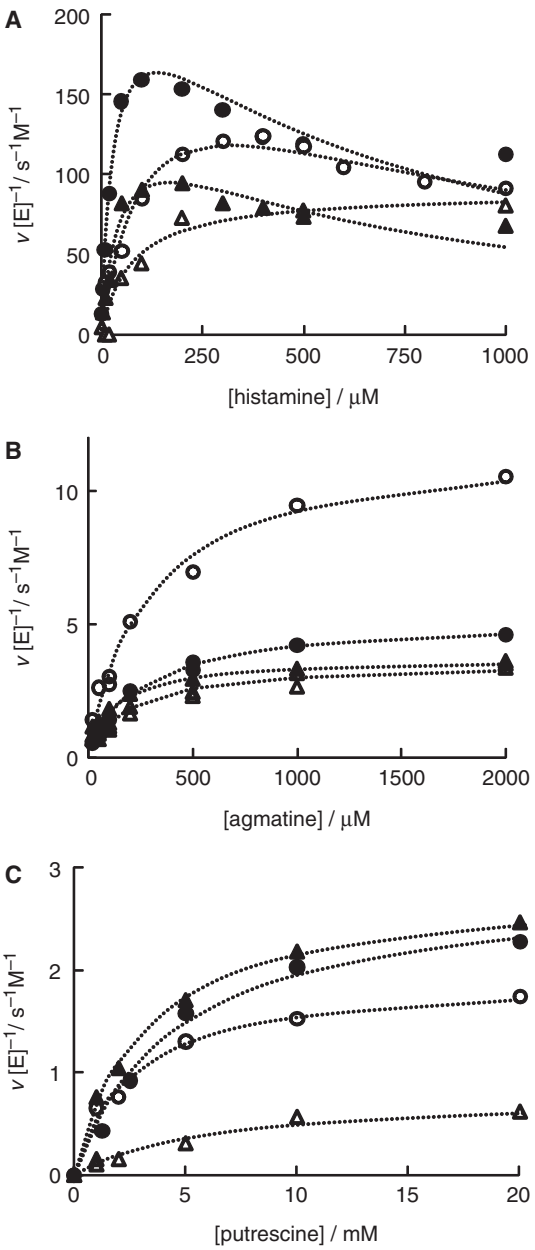

Fig. 2 Steady-state kinetic analysis of the reaction of WT, Y180F, G268D/D269C and Y180F/G268D/D269C nHmDH. (A) Histamine, (B) agmatine and (C) putrescine. Closed circles, data for recombinant wild-type nHmDH; open circles, data for Y180F; closed triangles, data for G268D/D269C; open triangles, data for Y180F/G268D/D269C. Curves were fitted using Eq. (1) representing uncompetitive inhibition.

susceptible to substrate inhibition giving a waved pattern dependence on the concentration similar to that of WT. Such substrate inhibition was partially weakened for the Y180F mutant (open circle) and almost completely suppressed in the Y180F/G268D/D269C mutant (open triangle), although the enzymatic activity itself was decreased. Agmatine and putrescine are poor substrates, and they exhibited standard saturation dependence of the kinetics on the substrate concentration for WT and the three mutants (Fig. 2B and C). The dotted lines in Fig. 2 represent the regression curves, and the refined enzyme kinetic parameters

Table 1. Steady-state enzyme kinetic parameters for wild-type and mutant nHmDHs with various amine substrates[a].

	WT	Y180F	G268D/D269C	Y180F/G268D/D269C
Histamine				
k_{cat} s^{-1}	2.5 (±0.1) × 10^2	2.0 (±0.1) × 10^2	1.5 (±0.1) × 10^2	8.9 (±0.1) × 10
K_S μmol	33 ± 2	1.2 (±0.1) × 10^2	50 ± 1	76 ± 1
k_{cat}/K_S s^{-1} μmol^{-1}	7.2 ± 0.1 (100)[b]	1.6 ± 0.2 (100)[b]	2.9 ± 0.1 (100)[b]	1.2 ± 0.1 (100)[b]
K_i μmol	5.8 (±0.1) × 10^2	8.3 (±0.4) × 10^2	5.9 (±0.1) × 10^2	∞
Agmatine				
k_{cat} s^{-1}	5.3 ± 0.2	12 ± 1	3.7 ± 0.8	3.5 ± 0.6
K_S μmol	2.4 (±0.1) × 10^2	2.8 (±0.1) × 10^2	1.2 (±0.1) × 10^2	1.9 (±0.1) × 10^2
k_{cat}/K_S s^{-1} μmol^{-1}	2.2 (±0.1) × 10^{-2} (0.31)[b]	4.3 (±0.3) × 10^{-2} (2.7)[b]	3.1 (±0.8) × 10^{-2} (1.1)[b]	1.8 (±0.2) × 10^{-2} (1.5)[b]
K_i μmol	∞	∞	∞	∞
Putrescine				
k_{cat} s^{-1}	2.8 ± 0.1	1.9 ± 0.1	2.8 ± 0.6	7.8 (±0.3) × 10^{-1}
K_S μmol	4.7 (±0.5) × 10^3	2.5 (±0.1) × 10^3	3.1 × 10^3	6.1(±0.2) × 10^3
$k_{cat}/K_S S^{-1}$ μmol^{-1}	6.0 (±0.4) × 10^{-4} (0.0083)[b]	7.6 (±0.4) × 10^{-4} (0.048)[b]	9.0 (±2.0) × 10^{-4} (0.031)[b]	1.3 (±0.1) × 10^{-4} (0.011)[b]
K_i μmol	∞	∞	∞	∞

[a]Reactions were performed in a 0.1 M potassium phosphate buffer, pH 7.5 at 30°C, and were initiated by the addition of Fc^+. Fc^+ concentration was 0.33 mM. [b]Numbers in parentheses represent the % ($k_{cat}K_S^{-1}$) versus histamine.

are summarized in Table 1. In the case of TMADH also, a pure substrate, diethylmethylamine, does not inhibit the enzyme activity even at high concentrations (*8*, *24*).

The inhibitory characteristics are well expressed by K_i. Both WT and G268D/D269C species have small K_i. The site-directed mutation of Tyr180 to Phe seems to be effective to reduce the substrate inhibition as observed as an increase in the K_i value in the Y180F mutation and more drastically in the Y180F/G268D/D269C mutation. However, all these mutation cause a decrease in the bimolecular rate constant between the free enzyme and the substrate, as judged from the k_{cat} K_S^{-1} values for histamine (Table 1). The k_{cat} value is also an important parameter which represents the rate constant of the forward decomposition of enzyme–substrate complex as well as enzyme–electron acceptor complex. The triple mutation as Y180F/G268D/D269C decreased k_{cat} significantly.

The comparison of the k_{cat} K_S^{-1} values for three substrates reveals that the mutation also induces the change in the substrate specificity. WT showed very high substrate specificity towards histamine as judged from the small k_{cat} K_S^{-1} values for agmatine and putrescine compared with that for histamine (Table 1). The three kinds of the mutation as Y180F, G268D/D269C and Y180F/G268D/D269C decreased the substrate specificity to some extents, as judged from the fact that the relative value of k_{cat} K_S^{-1} of agmatine against k_{cat} K_S^{-1} of histamine increased drastically by the mutation (Table 1).

UV-vis spectra of substrate-reduced nHmDH

Figure 3A shows the UV-vis absorption spectra of the oxidized and the histamine-reduced WT enzyme under anaerobic conditions at pH 7.5. The broad and strong absorption band with a maximum at 440 nm is assigned to $CFMN_O$ (Fig. 3A, dotted line). $CFMN_S$ gives two sharp absorption bands at 365 nm and 445 nm and one small broad band at around 500 nm, while $CFMN_R$ gives a broad absorption band with the maximum at around 360 nm (*9*). In the reductive half-reaction of the WT enzyme with histamine, two-electron reduction occurs per subunit at pH < 9 (*9*), and the two-electron-reduced WT gave the absorption bands at 365 and 445 nm at pH 7.5 (Fig. 3A, solid line), indicating the presence of $CFMN_S$. However, the absorption band (shoulder) at 445 nm was weak compared with that observed for one ultimate state containing $CFMN_S$ predominantly over $CFMN_R$. This means that part of the two-electron-reduced form of WT is in the other ultimate state containing $CFMN_R$.

On the addition of excess histamine (20-equivalent), the absorption bands at 365 and 445 nm were slightly sharpened, and the small broad absorption band appeared at around 500 nm (Fig. 3A, dashed line). All these results indicate an equilibrium shift from the $CFMN_R$-FeS_O state to the $CFMN_S$-FeS_R state under the conditions.

In the case of agmatine and putrescine, the absorption spectra of the two-electron-reduced form of WT did not change by the addition of excess substrate (20-equivalent) (Fig. 3B and C). The two-electron-reduced form of WT with putrescine gave a smaller absorption peak assigned to $CFMN_S$ than that observed with histamine and agmatine. The equilibrium in the two-electron-reduced form of WT is influenced by the substrate used. In this paper, the argument on the effect of the substrate will be minimized for simplicity.

Figure 4 illustrates the UV-vis spectra of the two-electron-reduced form as well as the oxidized form for the three mutants: Y180F, G268D/D269C and Y180F/G268D/D269C. The absorption spectra of the fully oxidized form are almost identical with that of WT, indicating that the electronic state of $CFMN_O$ remains practically unchanged on the mutation. In addition, the absorption spectrum of the two-electron-reduced form of G268D/D269C (Fig. 4B) is also almost identical to that of WT (Fig. 3), indicating the favoured equilibrium of the $CFMN_S$-FeS_R state rather than the

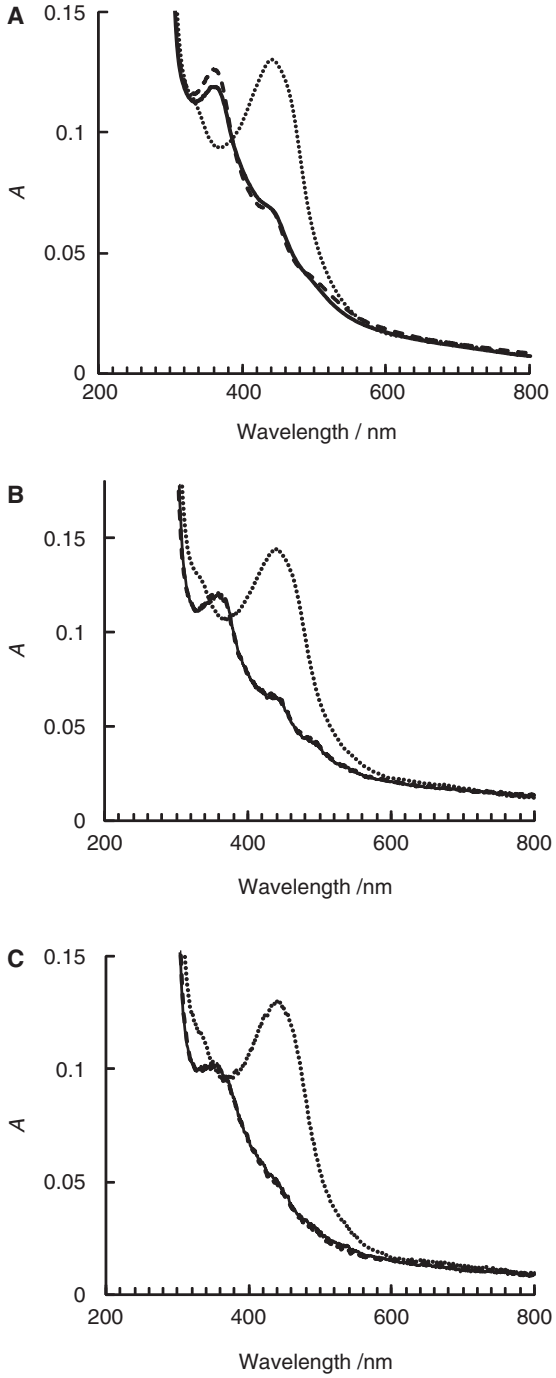

Fig. 3 UV-vis spectra of wild-type nHmDH with (A) histamine, (B) agmatine and (C) putrescine as substrates. Spectra of the oxidized (dotted line), substrate (2-equivalent amount)-reduced (solid line) and substrate (20-equivalent)-reduced wild-type nHmDH (dashed line) in a 0.1 M potassium phosphate buffer, pH 7.5.

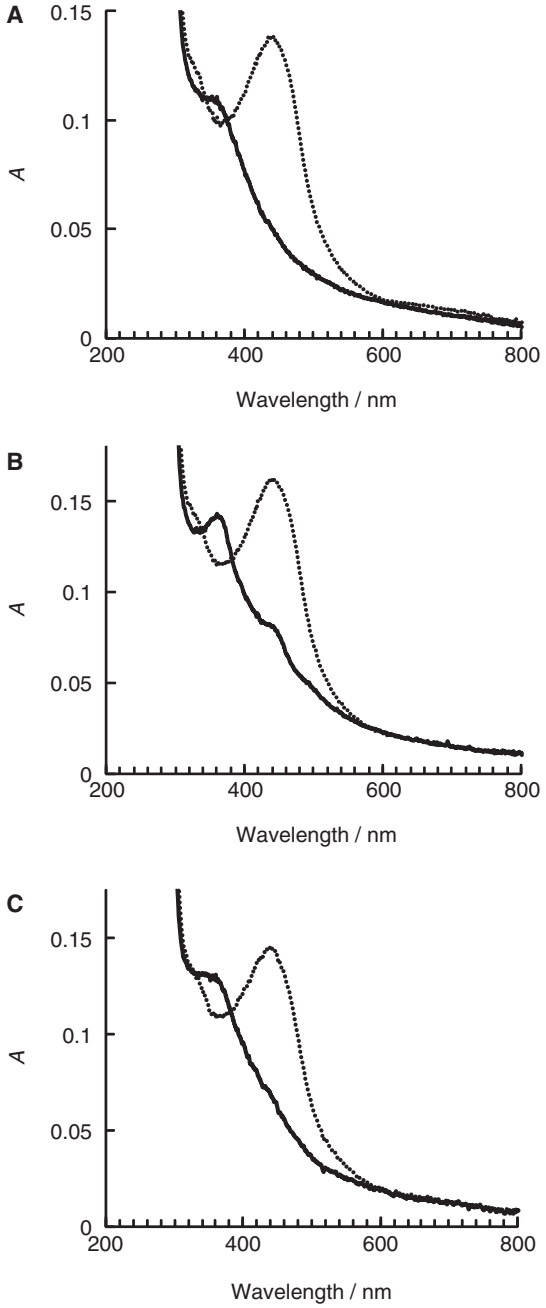

Fig. 4 UV-vis spectra of (A) Y180F, (B) G268D/D269C and (C) Y180F/G268D/D269C nHmDH. Spectra of oxidized (dotted line) and substrate-reduced (solid line) in a 0.1 M potassium phosphate buffer, pH 7.5, respectively.

$CFMN_R$-FeS_O state in the two-electron-reduced form at pH 7.5.

On the other hand, interestingly, the two-electron-reduced form of Y180F and Y180F/G268D/D269C did not give any absorption peak assigned to $CFMN_S$, but a board absorption band at around 360 nm assigned to $CFMN_R$ (Fig. 4A and C). This means that the equilibrium lies to the $CFMN_R$-FeS_O state in the two-electron-reduced form of the Y180F and Y180F/G268D/D269C mutants.

Evaluation of the redox potentials

In order to verify the equilibrium shift mentioned above, we attempted to evaluate the redox potential of the CFMN and [4Fe–4S] cluster in the enzymes. The CFMN cofactor is silent in direct electrochemistry but shows a characteristic absorption spectral change during the redox reaction (*9*, *25*). Therefore, a mediated spectroelectrochemical titration method is useful to evaluate the redox potential of CFMN (Fig. S1) (*9*).

Table 2. Redox potentials of the flavin and the [4Fe–4S] iron–sulfur cluster in nHmDH at pH 7.5.

	$E^{\circ\prime}_{O/S}$/mV[a]	$E^{\circ\prime}_{S/R}$/mV[a]	$E^{\circ\prime}_{O/R}$/mV[a]	$E^{\circ\prime}_{FeS}$/mV[b]	K_S^c	K_2^d
WT	16	0	8	23[e]	1.8	2.4
Y180F	–[f]	–[f]	27	−26	≪1	≪1
G268D/D269C	−138	−155	−146	−140	1.9	1.8
Y180F/G268D/D269C	–[f]	–[f]	20	37	≪1	≪1

[a]Evaluated potentials by mediated spectroelectrochemical titrations. [b]Midpoint potential determined by cyclic voltammetry using an ITO electrode. [c]Calculated values using Eq. (3). [d]Calculated values using Eq. (4). [e]Data taken from Tsutsumi *et al.* (2008). [f]Not determined.

Considering the existence of an intermediate $CFMN_S$ during the two-electron reduction of CFMN:

$$CFMN_O + e^- \leftrightarrows CFMN_S \qquad E^{\circ\prime}_{O/S} \qquad (2a)$$

$$CFMN_S + e^- \leftrightarrows CFMN_R \qquad E^{\circ\prime}_{S/R} \qquad (2b)$$

$$CFMN_O + 2e^- \leftrightarrows CFMN_R \qquad E^{\circ\prime}_{O/R}[= (E^{\circ\prime}_{O/S} + E^{\circ\prime}_{S/R})/2], \qquad (2c)$$

a two-step single-electron transfer model was adopted for the Nernstian analysis of the absorbance change at 365 nm and 440 nm (*9*). $E^{\circ\prime}_{O/S}$ and $E^{\circ\prime}_{S/R}$ as the redox potentials of Eqs. (2a) and (2b) as well as $E^{\circ\prime}_{O/R}$ as the redox potential of Eq. (2c) were thus evaluated and are summarized in Table 2.

The G268D/D269C mutation caused a drastic shift in $E^{\circ\prime}_{O/S}$ and $E^{\circ\prime}_{S/R}$ to the direction of the negative potential. In the case of the Y180F and Y180F/G268D/D269C mutant, we could not evaluate $E^{\circ\prime}_{O/S}$ and $E^{\circ\prime}_{S/R}$ separately, because no clear absorption band assigned to $CFMN_S$ was observed during the titration and the titration curve was simply analysed on a conventional one-step two-electron transfer model [Eq. (2c)]. The common property is ascribed to the thermodynamic instability of $CFMN_S$ in the overall redox reaction, that is, an extremely low value of the semiquinone formation constant (or comproportionation constant, K_S) defined by:

$$K_S = \frac{[CFMN_S]^2}{[CFMN_O][CFMN_R]} = \exp(F(E^{\circ\prime}{}_{O/S} - E^{\circ\prime}{}_{S/R})/RT), \qquad (3)$$

where F, R and T are the Faraday constant, the gas constant and the absolute temperature, respectively. The data suggest that the Y180F mutation is responsible for strong destabilization of $CFMN_S$, but details remain unknown.

On the other hand, the spectroscopic information of the [4Fe–4S] iron–sulfur cluster is not easy to extract. However, the [4Fe–4S] cluster in the enzyme can communicate directly with ITO electrodes and then cyclic voltammetry is available for evaluation of the redox potential of the [4Fe–4S] cluster, $E^{\circ\prime}_{FeS}$ (Fig. S2) (*9*, *25*). The data evaluated for the enzymes are summarized in Table 2. The large negative shift in $E^{\circ\prime}_{FeS}$ was observed for the Y180F and G268D/D269C mutants, but $E^{\circ\prime}_{FeS}$ of Y180F/G268D/D269C was close to that of WT at pH 7.5. The data indicate that $E^{\circ\prime}_{FeS}$ is also sensitive to the mutation even in the vicinity of CFMN, but the reason is not clear at this stage.

Discussion

The present work has shown that the site-direct mutations of Tyr180, Gly268 and Asp269 located in the vicinity of CFMN strongly affect the enzyme kinetics including substrate inhibition and substrate specificity, the spectroscopic property of two-electron-reduced form and the redox potential of the redox sites. The substrate inhibition from a natural substrate histamine has been successfully suppressed by the Y180F/G268D/D269C mutation, although the bimolecular rate constant between the enzyme and the substrate (k_{cat} K_S^{-1}) decreases to 17% of WT (Table 1). This seems to be reasonable in part, since the Y180F/G268D/D269C mutation was designed to imitate the amino acid sequence in the vicinity of the catalytic site of rHmDH, which does not suffer from the histamine inhibition. Interestingly, the k_{cat} K_S^{-1} value of rHmDH is only 23% of the WT nHmDH (unpublished data) and is close to that of the Y180F/G268D/D269C mutant. However, the decrease in the k_{cat} K_S^{-1}value is not simply responsible for the substrate inhibition-free characteristics, as evidenced by the enzyme kinetics of the G268D/D269C mutant, which shows the k_{cat} K_S^{-1}value of only 22% of WT but is susceptible to the histamine inhibition as in the case of WT.

The spectroscopic data suggest that the mutations examined here scarcely affect the electronic state of $CFMN_O$. However, the electronic state of the two-electron-reduced form of the enzyme is very sensitive to the mutation. The G268D/D269C mutant as well as WT contains obviously $CFMN_S$ in the two-electron-reduced form, but CFMN is fully reduced to $CFMN_R$ in Y180F and G268D/D269C mutants. The situation can be reasonably explained in view of thermodynamics as follows.

nHmDH is three-electron equivalent per subunit for full reduction, but the substrate can provide only two electrons per subunit at pH < 9 (*9*). Therefore, the substrate-derived two-electron-reduced form has two ultimate states: $CFMN_S$-FeS_R and $CFMN_R$-FeS_O. The distribution equilibrium is a function of $E^{\circ\prime}_{S/R}$ and $E^{\circ\prime}_{FeS}$:

$$K_2 \equiv \frac{[CFMN_S - FeS_R]}{[CFMN_R - FeS_O]} = \exp\left(\frac{F(E^{\circ\prime}_{FeS} - E^{\circ\prime}_{S/R})}{RT}\right). \qquad (4)$$

The K_2 value is about 2 for WT and G268D/D269C mutant as calculated from the value in Table 2, but that is close to 0 for the Y180F and G268D/D269C mutants. Note here that the $E^{\circ\prime}_{S/R}$ values of Y180F and G268D/D269C could not be evaluated here but should

be much positive than $E^{\circ\prime}_{O/R}$, since the semiquinone formation constant K_S is close to 0. Considering the enzyme kinetics and the thermodynamic argument as well as spectroscopic properties, it is reasonably concluded that large K_2 value (probably more than about unity) is responsible for the substrate inhibition.

Substrate inhibition is considered to be a special case of uncompetitive inhibition, and thus some interaction must exist between the enzyme in the substrate-reduced state and the substrate. The idea is supported by the spectral data in Fig. 3: the absorption peaks assigned to $CFMN_S$ of the two-electron-reduced form of WT becomes more evident in the presence of excess amount of histamine. There seems to be the plausible second binding site for the substrate. The site is not responsible for the enzyme catalysis, but the binding seems to perturb the redox potential to increase the K_2 value. Interestingly, such spectral perturbation in the two-electron-reduced form was observed in the G268D/D269C mutants on the addition of excess amount of histamine (data not shown) and similar spectroscopic phenomena are reported for TMADH (*8*). At high trimethylamine concentrations, the spectrum also exhibits a high absorption at 365 nm that is characteristic of the semiquinone form of the flavin (*8*).

The property of large K_2 value is strongly related to that of large K_S value, that is, $E^{\circ\prime}_{O/S} > E^{\circ\prime}_{S/R}$ (Table 2). Under such situations, the second step of the two sequential single electron transfers from the reduced flavin to the [4Fe–4S] cluster (that is, the single electron transfer from $CFMN_S$ to FeS_O) is not favoured compared with that of the first step electron transfer (the electron transfer from $CFMN_R$ to FeS_O) in view of the thermodynamics and then becomes one of the key steps to govern the k_{cat} value. The binding of the second substrate enhances the situation, which should reduce the enzyme kinetics. We believe that this is the situation explaining the substrate inhibition.

On the other hand, Y180F and G268D/D269C mutants did not show any spectral change on the addition of excess amount of histamine. The small perturbation of the redox potential induced by the second binding of the substrate, if any, might not be enough to bring $CFMN_S$ into existence for the Y180F and G268D/D269C mutants, because the K_2 value is too small before the second binding.

In contrast, the K_S and K_2 values of Y180F/G268D/D269C are much smaller than those of WT. Small K_2 value means uphill single electron transfer from the $CFMN_R$ to FeS_O. This situation is not convenient for fast enzyme turnover and k_{cat} should be small. The G268D/D269C mutation causes a decrease in the enzyme activity (decrease in k_{cat} and increase in K_S) (Table 1). This might also be explained in terms of the redox potential. The negative shift in $E^{\circ\prime}_{O/R}$ and $E^{\circ\prime}_{FeS}$ caused by the G268D/D269C mutation results in the decrease in the driving force of the reaction between the free enzyme and the substrate. In a similar way, the decrease in the enzyme activity by the Y180F might be ascribed to the positive shift of $E^{\circ\prime}_{O/R}$ and the negative shift of $E^{\circ\prime}_{FeS}$ (Table 2). The situation leads to the uphill electron transfer from CFMN to [4Fe–4S] cluster.

In conclusion, the amino acid residues in the vicinity of CFMN play very important role in governing the redox potential of CFMN and [4Fe–4S] cluster, and then the semiquinone formation constant K_S and the electron distribution constant K_2 between CFMN and the [4Fe–4S] cluster are easily influenced by the amino acid residues. The reason is not clarified in this work, but it has been found that the enzyme kinetics is very sensitive to the thermodynamic property. The substrate inhibition from histamine is strongly related to the stability of $CFMN_S$ in the two-electron-reduced form, as represented by large K_2. In contrast, however, small K_2 value leads to uphill single electron transfer from $CFMN_R$ to FeS_O, which results in the decrease in the kinetics. Because of the conflicting properties ascribed to the K_2 value, it seems to be very difficult to generate mutant enzymes with large $k_{cat}\ K_S^{-1}$ value without substrate inhibition. When we consider some application of the enzyme as catalysts of biosensors or bioassay of histamine, nHmDH with a large K_2 value is convenient for low concentration sample analysis because of large $k_{cat}\ K_S^{-1}$ value, while rHmDH with small K_2 value is convenient for high concentration sample analysis because the enzyme does not suffer from the substrate inhibition. The negative shift of $E^{\circ\prime}_{O/R}$ occurred in the G268D/D269C or that of $E^{\circ\prime}_{FeS}$ occurred in the Y180F also leads to the kinetic hindrance derived from the thermodynamic situation.

Supplementary data

Supplementary Data are available at *JB* Online.

Acknowledgement

The authors thank Kikkoman Corporation for their kind gift of rHmDH.

Funding

This work was supported in part by Grants-in-Aids for Scientific Research from the Ministry of Education, Science, Sports and Culture of Japan (to M.T. 20-3618 and to K.K. 15380082 and 19310070).

Conflict of interest

None declared.

References

1. Siddiqui, J.A., Shoeb, S.M., Takayama, S., Shimizu, E., and Yorifuji, T. (2000) Histamine dehydrogenase of *Nocardioides simplex*: a second bacterial enzyme for histamine degradiation. *J. Biochem. Mol. Bio. Biophys.* **5**, 37–43
2. Suddiqui, J.A., Shoeb, S.M., Takayama, S., Shimizu, E., and Yorifuji, T. (2000) Purification and characterization of histamine dehydrogenase from *Nocardioides simplex* IFO 12069. *FEMS Microbiol. Lett.* **189**, 183–187
3. Fujieda, N., Satoh, A., Tsuse, N., Kano, K., and Ikeda, T. (2004) 6-*S*-cysteinyl flavin mononucleotide-containing histamine dehydrogenase from *Nocardioides simplex*: molecular cloning, sequencing, overexpression, and characterization of redox centers of enzyme. *Biochemistry* **43**, 10800–10808

4. Limburg, J., Mure, M., and Klinman, J.P. (2005) Cloning and characterization of histamine dehydrogenase from *Nocardioides simplex*. *Arch. Biochem. Biophys*. **436**, 8–22
5. Huang, L., Rohlfs, R.J., and Hille, R. (1995) The reaction of trimethylamine dehydrogenase with electron transferring flavoprotein. *J. Biol. Chem*. **270**, 23958–23965
6. Jang, M.-H., Basran, J., Scrutton, N.S., and Hille, R. (1999) The reaction of trimethylamine dehydrogenase with trimethylamine. *J. Biol. Chem*. **274**, 13147–13154
7. Falzon, L. and Davidson, V.L. (1996) Kinetic model for regulation by substrate of intramolecular electron transfer in trimethylamine dehydrogenase. *Biochemistry* **35**, 2445–2452
8. Roberts, P., Basran, J., Wilson, E.K., Hille, R., and Scrutton, N.S. (1999) Redox cycles in trimethylamine dehydrogenase and mechanism of substrate inhibition. *Biochemistry* **38**, 14927–14940
9. Tsutsumi, M., Fujieda, N., Tsujimura, S., Shirai, S., and Kano, K. (2008) Thermodynamic redox properties governing half-reduction characteristics of histamine dehydrogenase from *Nocardioides simplex*. *Biosci. Biotechnol. Biochem*. **72**, 786–796
10. Bakke, M., Sato, T., Ichikawa, K., and Nishimura, I. (2005) Histamine dehysrogenase from *Rhizobium* sp.: gene cloning, expression in *Escherichia coli*, characterization and application to histamine determination. *J. Biotechnology* **119**, 260–271
11. Takagi, K. and Shikata, S. (2004) Flow injection determination of histamine with a histamine dehydrogenase-based electrode. *Anal. Chim. Acta* **505**, 189–193
12. Sato, T., Horiuchi, T., and Nishimura, I. (2005) Simple and rapid determination of histamine in food using a new histamine dehydrogenase from *Rhizobium* sp. *Anal. Biochem*. **346**, 320–326
13. Yamada, R., Fujieda, N., Tsutsumi, M., Tsujimura, S., Shirai, O., and Kano, K. (2008) Bioelectrochemical determination at histamine dehydrogenase-based electrodes. *Electrochemistry* **76**, 600–602
14. Steenkamp, D.J. and Beinert, H. (1982) Mechanistic studies on the dehydrogenases of methylotrophic bacteria. 1. The influence of substrate binding to reduced trimethylamine dehydrogenase on the intramolecular electron transfer between its prosthetic groups. *Biochem. J*. **207**, 233–239
15. Deakyne, C.A. and Meot-Ner, M. (1985) Unconventional ionic hydrogen bonds. 2. $NH^{+}\cdots\pi$. Complexes of onium ions with olefins and benzene derivatives. *J. Am. Chem. Soc*. **107**, 474–479
16. Bellamy, H.D., Lim, L.W., Mathews, F.S., and Dunham, W.R. (1989) Studies of crystalline trimethylamine dehydrogenase in three oxidation state and in the presence of substrate and inhibitor. *J. Biol. Chem*. **264**, 11887–11892
17. Barber, M.J., Neame, P.J., Lim, L.W., White, S., and Mathews, F.S. (1992) Correlation of X-ray deduced and experimental amino acid sequences of trimethylamine dehydrogenase. *J. Biol. Chem*. **267**, 6611–6619
18. Basran, J., Mewies, M., Mathews, F.S., and Scrutton, N.S. (1997) Selective modification of alkylammonium ion specificity in trimethylamine dehydrogenase by the rational engineering of cation-bonding. *Biochemistry* **36**, 1989–1998
19. Fujieda, N., Tsuse, N., Satoh, A., Ikeda, T., and Kano, K. (2005) Production of completely flavinylated histamine dehydrogenase, unique covalently bound flavin, and iron-sulfur cluster-containing enzyme of *Nocardioides simplex* in *Escherichia coli*, and its properties. *Biosci. Biotechnol. Biochem*. **69**, 2459–2462
20. Wilson, E.K., Mathews, F.S., Packman, L.C., and Scrutton, N.S. (1995) Electron tunneling in substrate-reduced trimethylamine dehydrogenase: kinetics of electron transfer and analysis of the tunneling pathway. *Biochemistry* **34**, 2584–2591
21. Segal, I.H. (1993) Uncompetitive inhibition in *Enzyme Kinetics*, pp. 136–143, Wiley-Interscience, New York
22. Tsujimura, S., Kuriyama, A., Fujieda, N., Kano, K., and Ikeda, T. (2005) Mediated spectroelectrochemical titration of proteins for redox potential measurements by a separator-less one-component bulk electrolysis methods. *Anal. Biochem*. **337**, 325–331
23. Nagabayashi, Y., Omayu, A., Yagi, S., Nakamura, K., and Motonaka, J. (2001) Evaluation of Osmium (II) complexes as electron transfer mediators accessible for amperometric glucose sensors. *Anal. Sci*. **17**, 945–950
24. Rohlfs, R.J. and Hille, R. (1994) The reaction of trimethylamine dehydrogenase with diethylmethylamine. *J. Biol. Chem*. **269**, 30869–30879
25. Tsutsumi, M., Tsujimura, S., Shirai, O., and Kano, K. (2009) Direct electrochemistry of histamine dehydrogenase from *Nocardioides simplex*. *J. Electroanal. Chem*. **625**, 144–148